- The full text is not change in any way.

The full-text must not be sold in any format or medium without the formal permission of the copyright holders.

The Design of Fault Tolerant Machines for Aerospace Applications

G.J. Atkinson, B.C. Mecrow, A.G. Jack, D.J. Atkinson

School of Electrical, Electronic and Computer Engineering, University of Newcastle upon Tyne, Newcastle upon Tyne NE1 7RU, UK, Tel (+44) 191-222-7340, Email G.J.Atkinson@ncl.ac.uk

P. Sangha, M. Benarous

Goodrich Corporation, Electromagnetic Systems Technical Centre, York Road, Birmingham B28 8LN, UK, Tel (+44) 121 627 6600

***Abstract* - This paper discusses the design of a fault tolerant electric motor for an aircraft main engine fuel pump. The motor in question is a four phase fault tolerant motor with separated windings and a six pole permanent magnet rotor. Methods of reducing machine losses in both the rotor and stator are introduced and discussed. The methods used to calculate rotor eddy current losses are examined. 3D finite element, 2D finite element time-stepping and 2D finite element harmonic methods are discussed and the differences between them and the results they produce investigated. Conclusions are drawn about the accuracy of the results produced and how the methods in question will help the machine designer.**

I. INTRODUCTION

An integrated electric main engine fuel pump in an aircraft has a number of potential benefits. The fuel control system will be lighter in weight, smaller, simpler and more efficient than conventional systems using a mechanically driven pump. Fuel flow within the engine can be matched precisely to the engine's operating conditions, rather than governed solely by the engine speed.

Previous research by a variety of authors [1-8] has been carried out on the concepts, development, building and testing of fault tolerant drives. The authors have developed a 16kW 15,000 revs/min 4-phase 6-pole permanent magnet fault tolerant electric drive, which has been tested on a main engine fuel pump [9]. This system is illustrated in Fig. 1 The next stage of research has concentrated on increasing the size and speed of this machine to 100kW and 20,000 revs/min [10]. This power level has been identified for a medium to large size aircraft. Initially the machine magnetic and electric loadings were held constant and the size of the machine was increased to give enough volume to provide the increased torque level. A scale comparison of the two machines is given in Fig. 2

Table I compares the measured losses in the 16kW machine and the calculated losses for the 100kW version of the machine. On calculating the losses for the re-scaled machine it has become evident that the efficiency will decrease and the balance of losses will change, with rotor eddy current loss becoming the dominant loss mechanism, contributing 43% of the total loss.

This paper will look into the methods used to reduce total loss to a more acceptable level and then concentrate on the modelling of rotor eddy current loss, comparing a harmonic approach and a time-stepping method for calculating this loss.

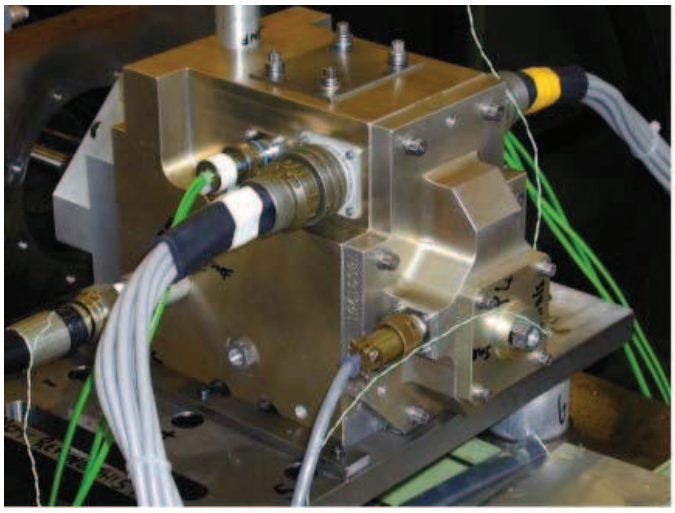

Fig. 1 16kW fault tolerant electric motor on test bed.

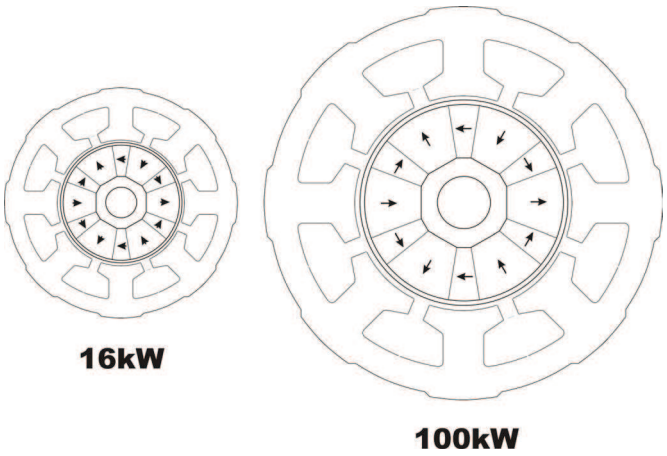

Fig. 2 Comparison between the 16kW and a 100kW fault tolerant motor

Table I. ELECTROMAGNETIC LOSSES FOR A 16KW AND A 100KW MACHINE.

Loss Mechanism	Loss as a percentage of output power	
	16kW machine	100kW machine
Full-load rotor loss	1.6%	7.9%
No-load losses	1.9%	5.9%
Full load winding loss	3.4%	4.4%
Total machine loss	**6.9%**	**18.3%**

II. DESIGN MODIFICATIONS TO REDUCE LOSS

Increasing the physical size and output power of the machine has resulted in a change in the amount and balance of losses, with rotor loss becoming dominant. Overall total machine losses have increased as a percentage of output power from 6.9% for a 16kW machine to 18.3% for a 100kW machine. Considerable effort has gone into designing a 100kW machine with a more acceptable efficiency. The steps taken to achieve this are discussed in this section of the paper.

A. Rotor eddy current loss

Non-synchronous air-gap magnetic fields induce eddy currents in the rotor. The loss due to these is significant for two reasons:

1) Each slot contains only one non-overlapping winding to ensure magnetic, electrical and thermal isolation is maintained to provide fault tolerance. This isolated winding arrangement results in a square air-gap MMF profile and consequently a high degree of non-synchronous air-gap harmonics.

2) The rotor is made using samarium cobalt magnets retained by a non-magnetic steel sleeve to withstand the centrifugal force of the magnets at high speed. Both of these materials are electrical conductors.

The air-gap harmonic spectrum can be altered by changing the stator design. The tooth pitch can be modified to increase the magnitude of the torque-producing 3rd harmonic (6 pole field), whilst decreasing the magnitude of the majority loss-inducing 5th harmonic. Fig. 3 illustrates the original stator design with equal wound and spacer tooth span and the altered design in which a reduction of 29% in rotor eddy current loss has been calculated [10].

The choice of magnet is somewhat limited by the thermal requirement of the machine, and the high centrifugal forces and machine environment limit the choice of rotor sleeve.

Rotor eddy current loss (particularly due to the high order harmonics) is reduced by increasing the air-gap length. This effectively reduces the depth to which the high order harmonics penetrate into the rotor, reducing the loss due to them.

B. Winding loss

On increasing the size, output power and speed of the fault tolerant machine, the number of turns has been reduced, when operating at the same supply voltage. Fewer but larger diameter conductors result in increased skin and proximity effects. Winding loss at full load and speed is now 4.4kW, seven times the equivalent DC winding loss.

Adoption of the new stator design in Fig. 3 encourages leakage flux to spread more into the slot, as shown in Fig. 4 This increases proximity loss. Along with this, the air-gap length has been increased to reduce rotor eddy current loss. This reduces the magnetic loading, requiring an increase in electrical loading to maintain the same output power, further exacerbating the problem.

With multi-stranded Litz type wire, consisting of fifteen ten strand conductors, a reduction in winding loss of 44% has been calculated. As shown in Table II, the a.c. loss is now only 21% greater than the d.c. loss.

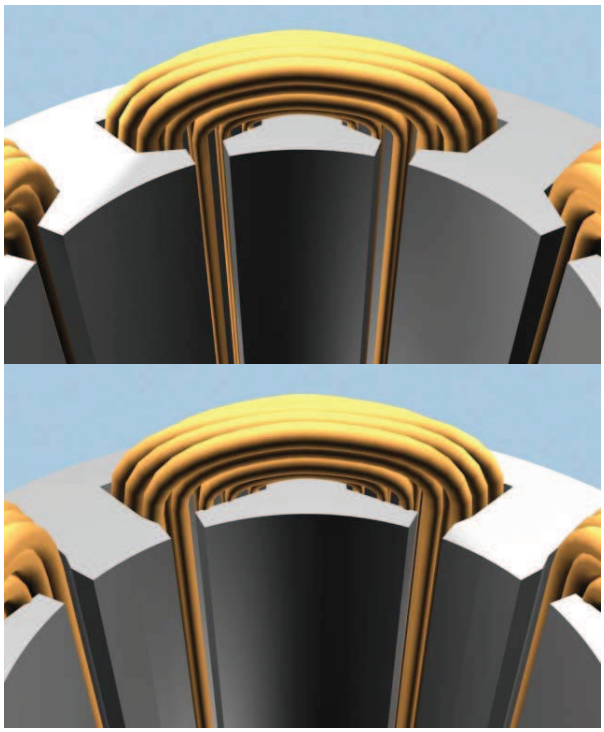

Fig. 3 Original and new stator design

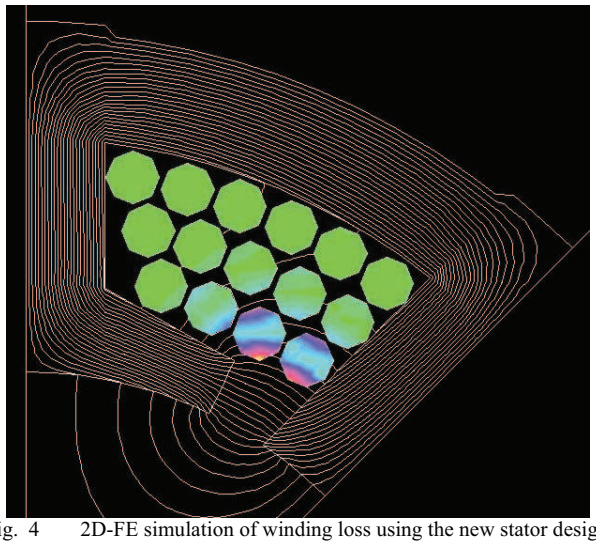

Fig. 4 2D-FE simulation of winding loss using the new stator design.

Table II. REDUCING WINDING LOSS

Winding type Stator design	**DC Loss (W)**	**AC Loss (W)**	**AC Loss / DC loss**
12 Solid Conductors Original stator design	621	4419	7.11
15 solid conductors New stator design	1323	7083	5.35
15 ten-strand conductors New stator design	2065	2492	1.21

C. No load loss

A series of tests carried out on the 16kW machine have separated winding loss, rotor eddy current loss and no-load loss [9]. As the name suggests, no-load loss is measured with the machine unloaded and open circuit, being driven by an external motor. The loss measured consists of viscous drag, stator iron and bearing loss.

The machine is fuel cooled by having the stator slots, core back and air-gap submerged in a flow of fuel. Fuel in contact with the rotor surface imposes a viscous drag loss on the machine. As shown in (1) the drag loss (M) is related to axial length (l_a), rotor outside diameter (r), speed (ω) and viscosity of the fuel (ρ). Flow of fuel is turbulent, with a high Reynold's Number. Consequently, the coefficient of friction is given by (2) with an air-gap length (l_g) and kinematic viscosity (μ).

$$M = C_f \pi r^4 l_a \rho \omega^2 \quad (1)$$

$$C_f = \frac{0.476 \times \sqrt[4]{\frac{l_g}{r}}}{\sqrt{\left(\rho \times \omega \times r \times l_g / \mu\right)}} \quad (2)$$

For the 100kW machine at 20,000 revs/min, drag loss comprises 80% of the no-load loss. This is reduced by decreasing the rotor outside diameter, and in turn increasing the air-gap length, which also reduces rotor eddy current loss. As drag loss is most heavily influenced by the rotor diameter, a reduction in rotor diameter from 76.8mm to 70mm results in a reduction in drag loss from 4.8kW to 2.7kW, a 44% reduction.

The most obvious way to reduce no-load iron loss is to use a thinner lamination steel. Iron loss is only 6.2% of total loss for this machine and increasing the total number of laminations by a factor of 3.5 will only shave a further 2.5% off total loss. The increased cost associated with more, thinner laminations far outweighs the benefits of reducing total loss by such a small amount.

D. Total machine loss

As shown in the previous section, reducing loss due to one mechanism can result in an increase in loss due to the other mechanisms. The designer must find the best compromise of the methods available to reduce total loss. The initial design is improved by reducing the rotor diameter, increasing the air-gap length, changing the stator tooth span and using multi-strand conductors. This reduces no-load, winding and rotor eddy current loss by a total of 35% as shown in Table III.

With rotor eddy current loss still the dominant source of loss, this paper will concentrate on the methods used in its calculation and the different results that arise depending on the calculation method used.

Table III. ELECTROMAGNETIC LOSSES FOR A 16KW AND A 100KW MACHINE.

Loss Mechanism	Loss as a percentage of output power	
	100kW initial design	100kW improved design
Full-load winding	4.4%	2.5%
No-load	5.9%	3.5%
Full-load rotor	7.9%	6.0%
Total	**18.3%**	**11.9%**

III. ROTOR EDDY CURRENT LOSS – TIMESTEPPING APPROACH

A. 3D modelling

Full knowledge of the time varying magnetic field distribution within the machine requires the use of 3D time-stepping finite element methods with movement incorporated into the mesh. Significant portions of the rotor loss result from small geometrical details such as the shape of the slot opening, and hence fine discretisation is required in these areas for an accurate result. The resultant problem is exceptionally large, and takes several days of computation to achieve a single solution. For this reason it is not a preferred design method except for final design verification. Approximations are generally made to reduce the model complexity.

B. 2D modelling

If the end effects are not significant, then rotor eddy current loss, along with other electromagnetic effects, can be calculated using two-dimensional finite element software, in which time-stepping is used in conjunction with moving surfaces. A two-dimensional finite element model of the 100kW machine was built with a rotating rotor, permanent magnet excitation, non-linear stator iron and sinusoidal winding currents. The model was set to run over four electrical cycles with 40 time steps per electrical cycle. The first cycle allows the solution to settle and the last three represent one complete mechanical revolution. A full field solution is produced at each time step. Fig. 5 illustrates a example instantaneous flux distribution with rotor eddy current loss density superimposed.

Both instantaneous and time domain results can be obtained for rotor eddy current loss, flux density at a position, magnetic field strength on a surface and output torque. Rotor eddy current loss is made up of both loss due to the MMF asynchronous harmonics and loss due to flux perturbations caused by the magnets moving beneath a slot opening and then a tooth.

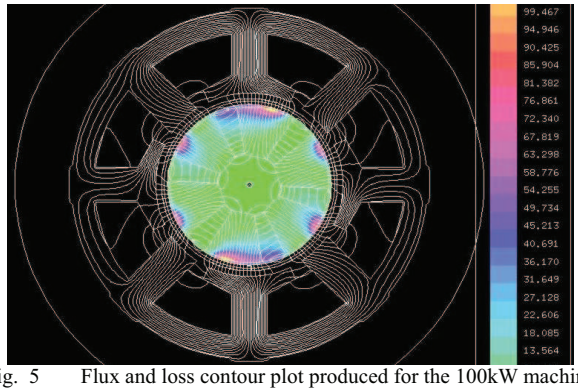

Fig. 5 Flux and loss contour plot produced for the 100kW machine using a time-stepping method.

IV. ROTOR EDDY CURRENT MODELLING – HARMONIC APPROACH

An alternative approach to this all-in-one method is to look solely at rotor eddy current loss using a simplified harmonic approach. Rotor eddy current loss is due to changes in the air-gap magnetic field. When viewed from the rotating rotor, this field is alternating in both time and space and has a complex waveform. The harmonic approach sums the effect of each individual harmonic as seen from the rotor.

The air-gap tangential magnetic field strength is defined by the rate of change of MMF with respect to position. The peak magnetic field occurs at the slot openings where the tangential magnetic field strength is the greatest and is virtually zero elsewhere. The harmonics of this field are found by Fourier de-composition. This operation gives the air-gap harmonic spectrum shown in Fig. 6

Torque is produced by the interaction of the 6-pole rotor and stator fields, or 3rd air-gap harmonic. This torque-producing harmonic is locked onto the rotor and as such induces no rotor eddy current loss. All other harmonics are asynchronous with the rotor and rotate alternately backwards and forwards at ever increasing speeds with respect to it. It is the eddy currents induced by these asynchronous fields which cause the rotor eddy current loss that has become an issue with this type of machine.

In an interesting approach adopted in [11-13] an analytical solution based upon a similar harmonic approach has been developed. However, for this application the range of design options included the use of highly conducting screens, in which the currents are skin limited. The authors were also examining segmentation schemes for the magnet assembly (for which analytical solutions are not appropriate) and therefore chose to adopt a 2D finite element approach to the solution.

A 2D FE simulation was carried out, with each harmonic applied separately to a small section of the rotor. Periodic boundaries were used to limit the extent of the problem. Fig. 7 illustrates this for the 15th harmonic.

The 2D FE model of the rotor segment with field applied was solved for a known field strength. The bulk of the eddy currents occur within the magnet and sleeve, which have a linear magnetic permeability. Eddy current loss is consequently proportional to the field magnitude squared, so eddy current loss can be calculated for any field magnitude with this scaling factor once a set of results with a known field magnitude have been generated. The effect of changes in electrical loading can then be found without running a new FE simulation. Changes to the tooth span and slot opening of the stator, which affect only the harmonic spectrum, can also be investigated by applying the correct magnitude for each harmonic.

Changes in rotor or stator diameter, air-gap size, rotational frequency and rotor materials will require a new FE model to be built and simulated which is a quick process for such a small model. When the 2DFE simulation was carried out and the correct magnitude for each harmonic applied, the rotor eddy current loss spectrum shown in Fig. 8 was produced.

The majority of loss is due to eddy currents induced by the 1st harmonic (2-pole field). This was not the case, however, for the original 100kW machine design based on the 16kW machine design. With the original stator tooth layout and slot opening size, the majority of rotor eddy current loss was due to the 5th air-gap harmonic (10-pole field) [10]. This information indicated that a re-design of the stator tooth width was required to reduce the excessive rotor losses. The effect of this change was found by simply producing a new Fourier series and applying the magnitude of each harmonic to the already generated FE results with the scaling factor applied to take account of the difference between the simulated and actual harmonic field magnitude. This procedure indicated a 13% reduction in total rotor eddy current loss and an increase in machine torque. With the electrical loading dropped to bring the torque back to its rated value, the reduction in rotor eddy current loss became 29%. This change to the machine design is revealed by the harmonic method but would not be so evident with the time-stepping approach.

V. COMPARISON BETWEEN THE TWO METHODS

The same machine design has been simulated at full speed and full load using the two methods described. Table IV summarises the amount of rotor eddy current loss calculated by each method.

A 10% difference exists, with the time-stepping method providing a lower value for total loss when compared to the results from the harmonic method.

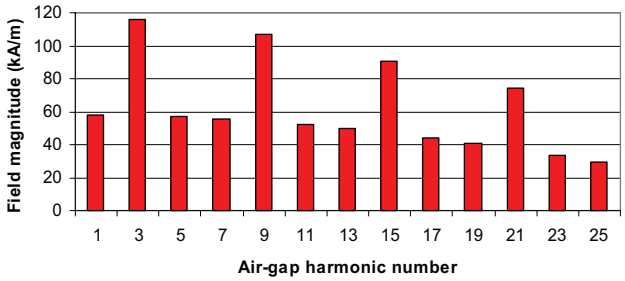

Fig. 6 Air-gap tangential magnetic field spectrum of the 100kW machine

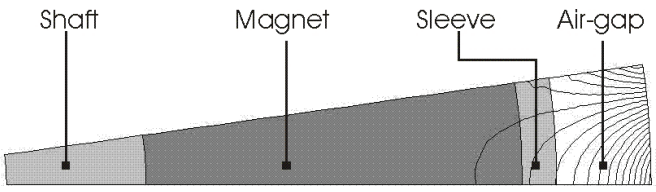

Fig. 7 2DFE model of the 15th harmonic applied to a section of the rotor

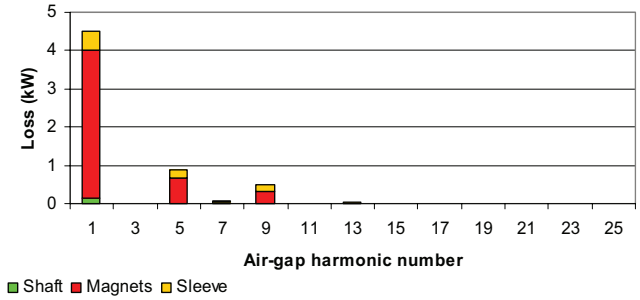

Fig. 8 Rotor eddy current loss spectrum

Table IV. ROTOR EDDY CURRENT LOSS CALCULATED VIA A HARMONIC AND A TIME STEPPING APPROACH

Source of loss	Finite element calculated loss in Watts		Percentage difference
	Harmonic method	Time step method	
Magnets	4937	4488	-9%
Sleeve	904	824	-9%
Shaft	143	67	-53%
Total loss	**5984**	**5379**	**-10%**

A. Rotor Loss Composition

The harmonic loss method revealed that the majority of rotor eddy current loss is due to the 1st harmonic (2-pole asynchronous field). This can also be seen in the results from the time stepping method as shown in Fig. 9 This is a shade plot of rotor eddy current loss density. A diametrically opposite region of high loss can be seen in the rotor. Since these regions are 180 degrees apart, the high loss region must be due to the 1st harmonic.

B. The Effect of Non-Linearity

In the time stepping model the stator iron is modelled with a B/H curve to represent non-linearity, whereas in the harmonic method the stator iron is assumed infinitely permeable. There will be an MMF drop in the core which is not taken account of in the harmonic method and to consider this effect, the time stepping model was run with a linear and very high permeability stator. A slight increase in rotor loss from 5379W to 5459W was found when compared to the non-linear case. Clearly, saturation of the stator does not have a significant impact upon rotor eddy current loss.

C. Harmonic spectrum

The harmonic approach uses the Fourier series calculated for the ideal case, where the tangential field strength is assumed to be constant across each stator slot opening. This profile is shown in the red trace in Fig. 10 . It is of interest to compare this ideal field profile with that obtained from the slot in the time-stepping model.

With the magnets de-magnetised (as is the case in the harmonic method model) the magnetic field strength profile generated by the time-stepping approach is spread beyond the slot and has a lower magnitude than the ideal case (the blue trace). This spreading is due to the limited amount of elements placed in the region of the slot.

A more exact case is shown by the orange trace, (this can be derived analytically or using a magneto-static model of the slot with many elements in the slot and infinitely permeable iron). It is clear that the idealised case adopted by the harmonic model is closer to the exact case than that taken from the time-stepping model, simply because the time-stepping model would require a huge number of elements in order to give a more accurate model.

It is easy to see that the smoothed profile from the time-step model will have lower magnitude high order harmonics. This is evident when the amount of rotor loss is calculated using its harmonics and the harmonic eddy current loss method. This result is compared to the eddy current loss due to the idealised case harmonics and shown in Table V.

Table V. ROTOR EDDY CURRENT LOSS OBTAINED USING THE HARMONIC METHOD AND THE SPECTRA FROM THE IDEAL SLOT FIELD PROFILE AND THE TIMESTEP MODEL SLOT FIELD PROFILE.

Field Profile	Harmonic method 2DFE calculated Loss (W)		
	1st harmonic	High order harmonics	Total
Ideal	4499	1485	5984
Timestep	4746	1253	6000

D. Tooth ripple loss

Tooth ripple loss occurs because of rotor flux perturbations caused as the magnets pass beneath a slot opening and then a tooth. This effect is implicitly included when using a time stepping method as the magnets, slots, teeth and movement are all included in the model. Tooth ripple loss can be separated from the total MMF harmonic losses by running the simulation with the currents turned off. All eddy currents are then due to this flux perturbation, or tooth ripple as it is often known. For a machine such as the one described here, the large air-gap (5mm) results in small mean ripple loss of 44W. In addition to the mean loss the tooth ripple adds a harmonic as illustrated in the full-load time-stepping result in Fig. 11 By way of a comparison, the model was also run with the magnets de-magnetised. Fig. 12 illustrates how the harmonic is removed and the result settles into a constant loss as expected.

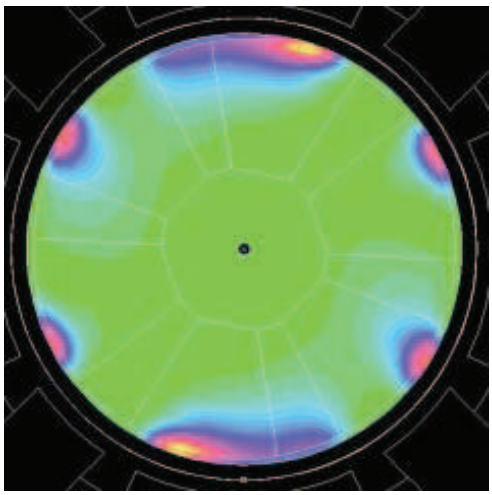

Fig. 9 Rotor eddy current shade plot.

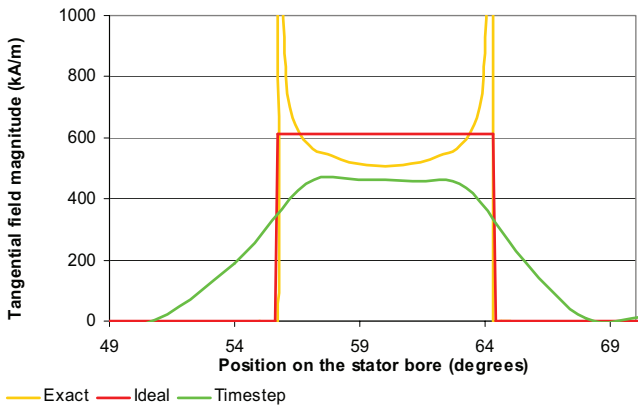

Fig. 10 Tangential field profile at the slot opening.

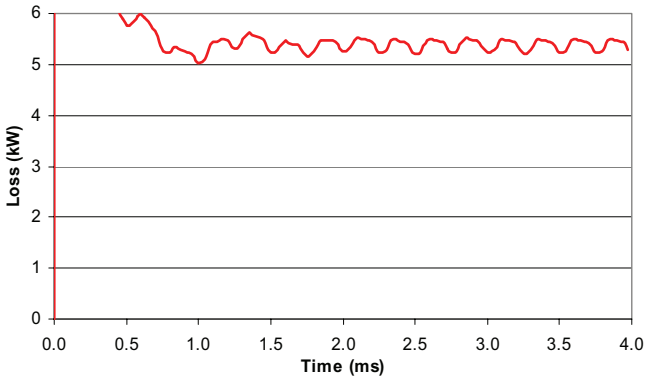

Fig. 11 Total loss against time with the magnets on.

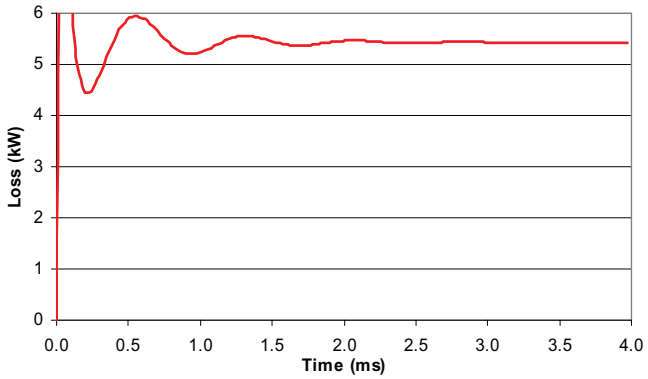

Fig. 12 Total loss against time with the magnets off.

E. 3D Solid Rotor Effects

The previous models discussed are in two dimensions only. In reality account must be taken of the extra path length the circulating eddy currents must follow at the ends of the rotor. This is illustrated in Fig. 13

The ratio of eddy current axial path length to eddy current rotor end path length is dependent on the order of the harmonic. Eddy currents due to the low order harmonics are current forced and have an additional 40% added to their path length due to the ends of the rotor. The effect of this is an increase in loss due to the low order harmonic.

High order harmonics have been found to be voltage forced and the increase in path length reduces these eddy currents and the losses due to them.

Table VI summarises the change resulting for the various harmonics when this path length adjustment is used [14]. For verification a full 3D, non-linear, moving rotor time-step FE model was created. Four days of computation time was required to simulate a single load condition. The total rotor loss was found to be 7540W. By comparison the 2D harmonic result with the empirical factor added gave a total rotor loss of 7706W (a 2% difference). This only required a few seconds of computation.

The harmonic method allows the effect of the end of the rotor to be added easily, whereas if a time-stepping method were used the loss due to each harmonic, and the different effect of the low and high-order harmonics would be hidden. As such an end effect correction could not be added. If the effect of the end of the rotor was required, a full 3D model would need to be constructed and, as discussed earlier, a single solution would take several days to solve.

Table VI. 2DFE CALCULATED LOSSES USING THE HARMONIC METHOD WITH END CORRECTION ADDED.

	Rotor eddy current loss (W)	
Harmonic	**2D harmonic model without end correction**	**2D harmonic model with end correction**
1st	4499	6300
5th	869	812
7th and higher	616	594
Total Loss	**5984**	**7706**

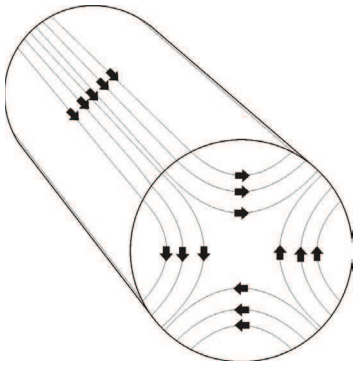

Fig. 13 Eddy current path in a solid rotor. [14]

VI. CONCLUSIONS

Increasing the physical size of the 16kW fault tolerant machine to achieve a 100kW power level has resulted in a reduction in efficiency and a change in the balance of machine losses, with rotor eddy current loss becoming the dominant loss mechanism. To achieve a more acceptable level of efficiency rotor eddy current loss is first investigated. To do this a method of calculating rotor eddy current loss which is both accurate and yields rapid results is required to investigate the effect design modifications have.

Full knowledge of the time varying magnetic field distribution within a machine requires the use of 3D time-stepping finite element methods, with movement incorporated into the mesh. During the investigative stage of a machine design, such an approach is inconvenient, as a single solution may take several days to solve.

Another approach is to use a 2D time-stepped model. Such a model will give a solution within the hour; however care must be taken in its construction as the results gained may not be as accurate as is required due to discretisation limitations. Investigation of design changes will also require a new mesh and solution. End effects are difficult to incorporate.

An alternative approach is to use a harmonic method. Using a harmonic approach in calculating rotor eddy current loss allows the designer to see which harmonics are causing the majority of the loss and take appropriate action. Knowing that a certain harmonic is causing the majority of the loss allows investigation into what changes can be made to the machine design, such as changing the tooth span and slot opening size. By recalculating the air-gap Fourier series and

applying this result to a set of pre-calculated 2DFE results, the effect of such a change on the machine design can be rapidly seen. Rotor eddy current loss due to the rotor end region can then be added as an empirical factor and again this result can be rapidly seen without the need to build a 3DFE model. Having the ability to analyse changes to the design of a machine in such a way is of great benefit to the designer and will allow faster development toward a final design.

Rotor eddy current, no-load and winding loss cannot be treated in isolation as modifying the machine design to reduce loss due to one, often results in increasing loss due to the others. Changing the stator design has reduced rotor eddy current loss by decreasing the magnitude of the loss inducing 5^{th} harmonic. Increasing the air-gap length, by reducing the rotor radius, has reduced rotor eddy current loss due to the high-order air-gap harmonics and no-load loss, as viscous drag loss is most heavily dependant on the rotor radius. However this has reduced the magnetic loading and the output torque of the machine. The torque level is restored by increasing the electrical loading, increasing winding loss. Winding loss is then reduced by using a multi-strand conductor.

Overall a 35% reduction in calculated loss is achieved when compared to the original 100kW machine design.

The final design is now under construction.

ACKNOWLEDGMENT

Testing of the 16kW fault tolerant fuel pump on a fuel pump test rig was carried out by the Goodrich Corporation, Engine Control Systems, Birmingham, UK.

Harmonic method 2DFE results were calculated using an in-house program developed by the Power Electronics, Drives and Machines Group at the University of Newcastle, UK. The 2D and 3D FE time-step results were produced using the MEGA program developed by the Applied Electromagnetic Research Centre at Bath University, UK and used at the Goodrich Corporation, Electromagnetic Systems Technical Centre, UK.

REFERENCES

[1] Richter, E., "Switched Reluctance Machines for High Performance Operations in a Harsh Environment - A Review Paper", Proc. ICEM Conf., Boston, 1990.

[2] Miller, T.J.E., 'Faults and Unbalanced Forces in the Switched Reluctance Machine', IEEE Transactions on Industry Applications, Vol. 31, No. 2, March/April 1995, pp. 319-328.

[3] Jack, B.C. Mecrow, and J. Haylock, ' A Comparative Study of Permanent Magnet and Switched Reluctance Motors for High Performance Fault Tolerant Applications', IEEE Transactions on Industry Applications, vol. 32, no. 4, July/August 1996, pp. 889-895.

[4] Jack, A.G., Mecrow, B.C. 'Safety critical Drives for Aerospace Applications'. Proceedings of the ICEM 1994, Paris, Vol. 1, pp. 91-96

[5] Jahns, T.M., 'Improved Reliability in Solid State AC drives by means of multiple independent phase-drive units', IEEE Trans, May 1980, IAS-16, (3), pp. 321-331

[6] Mecrow, B.C., Jack, A.G. and Haylock, J.A., "Fault Tolerant Permanent Magnet Machine Drives", IEE Proceedings, Part B., November 1996.

[7] Haylock, J.A., Mecrow, B.C., Jack, A.G., and Atkinson, D.J., "On-Line Detection of Winding Short-Circuits in Inverter Fed Drives", 9th International Conference on Electrical Machines and Drives, EMD'99, Christ Church College, Canterbury, 1-3 Sept. 1999, pp258-262.

[8] Haylock, J.A., Mecrow, B.C., Jack,A.G., and Atkinson, D.J., 'Operation of Fault Tolerant Machines With Winding Failures', IEEE International Electric Machines and Drives Conference, 1997.

[9] Mecrow, B.C., Jack, A.J., Atkinson, D.J., Green, S., Atkinson, G.J., King, A., Green, B. 'Design and Testing of a 4 Phase Fault tolerant Permanent Magnet Machine for an Engine Fuel Pump' IEE International Electrical Machines and Drives conference, 2003.

[10] Atkinson, G.J. Mecrow, B.C. Jack, A.G. Atkinson, D.J. Green, B. 'The influence of Stator Design on the performance of Fault Tolerant Machines' 16th international Conference on Electrical Machines, Krakow, Poland, 2004.

[11] Atallah, K. Howe, D. Mellor, P.H. Stone, D.A. 'Rotor Loss in permanent-Magnet Brushless AC Machines' IEEE Transactions on industry applications, Vol 36, No 6, Nov/Dec 2000 pp1612-1617

[12] Hiroaki, T. Xia, Z. Wang, J. Atallah, K. Howe, D. 'Rotor Eddy-Current Loss in Permanent magnet Brushless Machines' IEEE Transactions on Magnetics, Vol 40. No. 4, July 2004, pp2104-2106

[13] Ede, J.D. Atallah, K. Wang, J. Howe, D. 'Effect of Optimal Torque Control on Rotor Loss of Fault-Tolerant Permanent Magnet Brushless Machines' IEEE Transactions on magnetics, Vol 38, No 5, 2002 pp3291-3293

[14] Yee, H. 'Effects of Finite Length in Solid Rotor Induction Machines' Proc IEE, Vol 118, No 8, 1971, pp1025-1033